Environmental Science and Pollution Research (2024) 31:29434–29448
https://doi.org/10.1007/s11356-024-33131-1

RESEARCH ARTICLE

Adsorption properties and mechanism of Cu(II) on virgin and aged microplastics in the aquatic environment

Chun Hu[1] · Yaodong Xiao[1] · Qingrong Jiang[1] · Mengyao Wang[1] · Tingdan Xue[1]

Received: 20 November 2023 / Accepted: 25 March 2024 / Published online: 5 April 2024

Abstract

Microplastics (MPs) migrate by adsorbing heavy metals in aquatic environments and act as their carriers. However, the aging mechanisms of MPs in the environment and the interactions between MPs and heavy metals in aquatic environments require further study. In this study, two kinds of materials, polyamide (PA) and polylactic acid (PLA) were used as target MPs, and the effects of UV irradiation on the physical and chemical properties of the MPs and the adsorption behavior of Cu(II) were investigated. The results showed that after UV irradiation, pits, folds and pores appeared on the surface of aged MPs, the specific surface area (SSA) increased, the content of oxygen-containing functional groups increased, and the crystallinity decreased. These changes enhanced the adsorption capacity of aged MPs for Cu(II) pollutants. The adsorption behavior of the PA and PLA MPs for Cu(II) conformed to the pseudo-second-order model and Langmuir isotherm model, indicating that the monolayer chemical adsorption was dominant. The maximum amounts of aged PA and PLA reached 1.415 and 1.398 mg/g, respectively, which were 1.59 and 1.76 times of virgin MPs, respectively. The effects of pH and salinity on the adsorption of Cu(II) by the MPs were significant. Moreover, factors such as pH, salinity and dosage had significant effects on the adsorption of Cu(II) by MPs. Oxidative complexation between the oxygen-containing groups of the MPs and Cu(II) is an important adsorption mechanism. These findings reveal that the UV irradiation aging of MPs can enhance the adsorption of Cu(II) and increase their role as pollutant carriers, which is crucial for assessing the ecological risk of MPs and heavy metals coexisting in aquatic environments.

Keywords Microplastics · Aging · Cu(II) · Adsorption Mechanism · Heavy metals · UV irradiation

Introduction

Plastic products are a kind of high-quality polymer materials with light weight, low cost, strong plasticity and durability. They are widely used in aerospace, military, agriculture, industry, daily life and other fields (Tan et al. 2020). According to statistics, global plastic manufacturing will reach 367 million tons by 2020 (Chen et al. 2023), and by 2050, the global plastic output is expected to reach 34 billion tons (Petersen and Hubbart 2021). Despite their huge production, only 6 to14% of plastics are recycled (Alimi et al. 2018), and other plastics enter the environment in different ways. Plastic fragments or particles < 5 mm in diameter are generally referred to as MPs (Thompson et al. 2004). According to the different formation conditions, MPs can be divided into primary MPs and secondary MPs(Cole et al. 2011, Oni and Sanni 2022). Primary MPs are mainly micron and nano-scale plastic particles produced during the production, use and discharge of cosmetics and personal care products(Napper et al. 2015; Zhang et al. 2017). Secondary MPs are mainly produced by the crushing of large plastic fragments(Kataoka et al. 2019; Li et al. 2020). Most of the plastics that enter the environment will gradually break into smaller plastic fragments due to weathering, mechanical crushing, ultraviolet radiation, chemical reactions, microbial degradation and other environmental effects (De Gisi et al. 2022; Lionetto et al. 2023). The main types of MPs in the environment are polyethylene (PE), polypropylene (PP), polystyrene (PS), polyvinyl chloride (PVC), polyamide (PA), polyethylene terephthalate (PET), polylactic acid (PLA),

Responsible Editor: Tito Roberto Cadaval Jr

✉ Chun Hu
huchun1980@126.com

[1] School of Chemical and Environmental Engineering, Wuhan Polytechnic University, Wuhan 430023, People's Republic of China

polyurethane (PU) and nylon (Rayon) (Guo and Wang 2019, Rochman et al. 2013, Zhao et al. 2018).

MPs are pollutants that are widely distributed in environmental media such as oceans, rivers, lakes, sediments, and soils (Fiore et al. 2022; Hu et al. 2021; Li et al. 2018, 2021; Shen et al. 2018), and are even found in polar areas (Bergmann et al. 2019; Ding et al. 2023). MPs also entered the food chain (Wang et al. 2021a), and are enriched in organisms with higher trophic levels. Humans ingest MPs through diet, respiration, or skin contact, which can harm human health (Carbery et al. 2018; Rubio et al. 2020), which also presents an immense risk to ecological environmental security and biodiversity (Rahman et al. 2021). Compared with large plastics, MPs have a small particle size, high SSA, and high hydrophobicity, are difficult to degrade (Leng et al. 2023; Liu et al. 2018; Oni et al. 2020), and readily serve as carriers to adsorb and enrich various organic compounds, heavy metals, and microorganisms from external phases (Ahechti et al. 2022; Torres et al. 2021; Upadhyay et al. 2022). These pollutants also enter the food chain with MPs, and are transmitted and enriched between food chains, posing a serious risk to human wellness (Luo et al. 2023, Zhuang and Wang 2023). MPs help pollutants migrate into the environment through water transport or atmospheric flow, and can also interact with pollutants to produce combined effects, causing joint toxicity to organisms and ecosystems (Lv et al. 2022; Mejías et al. 2023). Consequently, the high concentrations of MPs in the environment and their associated environmental risks have attracted global attention in recent years.

In the natural environment, UV irradiation, thermal radiation, physical wear, chemical oxidation and biodegradation can cause different degrees of aging of MPs (Lang et al. 2020; Liu et al. 2020; Wang et al. 2021c). The aging process changes the physical and chemical properties of MPs, such as their surface morphology, functional group composition, crystallinity and hydrophobicity (Wright et al. 2013), thus affecting the adsorption capacity and adsorption mechanism of MPs for other pollutants. For example, studies have found that after aging, the surface of MPs becomes rough and cracks and gullies appear (Liu et al. 2019), the SSA and pore structure of particles increase (Fan et al. 2021b), and the oxygen functional groups on the surface of MPs also increase (Brennecke et al. 2016; Kalcíková et al. 2020), thereby increasing the binding sites on the surface of MPs (Wang et al. 2023), enhancing the adsorption capacity of pollutants and causing greater ecological and environmental risks.

Because of the rapid socioeconomic development and ongoing growth of metal electroplating, fertilizer manufacturing, mining, paper manufacture, and other industries, heavy metal ion-containing wastewater is being released into the environment in increasing amounts (Dong et al. 2019; He et al. 2020a; Wu et al. 2020; Xie et al. 2022), which makes the combined pollution of heavy metal ions and MPs serious. Among them, Cu(II) is the most common heavy metal pollutant discharged into water (Cherono et al. 2021; Wang et al. 2021b). Heavy metals have the characteristics of environmental persistence, biological concentration, undegradability and toxicity (Sheng et al. 2022; Velusamy et al. 2021), which can cause harm to human health and ecosystems at very low concentrations (O'Connor et al. 2020). MPs have high affinity for heavy metals in the aquatic environments and are good carriers of heavy metal ions (Foshtomi et al. 2019; Marsic-Lucic et al. 2018). Their adsorption capacity is affected by their own physical and chemical properties, such as morphology, SSA and aging degree (Luo et al. 2022). Recently, the reciprocity between heavy metals and MPs has attracted considerable attention from the academic community. The adsorption of heavy metal ions by MPs may enhance their environmental mobility, bioaccumulation and ecological risk (Khalid et al. 2021). The foundation for disclosing the environmental behavior and dangers of MPs and coexisting heavy metal ions in a combined contaminated aquatic environment to delineate the interaction strength and mechanism between MPs and coexisting heavy metal ions.

PA is a conventional plastic. Due to its good mechanical properties, heat resistance and chemical stability, it is widely used in automobiles, electronic appliances, machinery, rail transit, and sports equipment (Crespo et al. 2019; Reinaldo et al. 2020). PLA is a transparent and environmentally friendly biodegradable material with high strength, high modulus, and excellent formability and has great application value in various fields (Geng et al. 2020; Sun et al. 2022). PA and PLA MPs have been detected in several aquatic environments (Jang et al. 2020; Naji et al. 2021; Obbard et al. 2014; Yan et al. 2019). At present, investigations of MPs in the environment have mainly focused on original MPs, whereas the carrier effect of aged MPs remains to be studied. Therefore, two types of polymer particles with different functional groups, PA and PLA, were used as the target MPs in this study. Cu(II) was selected as the coexisting MPs pollutant with the highest detection rate in the aquatic environments.

Recent studies have shown that although aging has changed the adsorption of pollutants by MPs, the relationship between the characteristics of UV aging and the adsorption of heavy metals by MPs is still unclear. In order to fully understand the interaction between different types of MPs and Cu(II), it is necessary to consider the effects of aging process and different environmental conditions. Therefore, the adsorption behavior of Cu(II), a heavy metal pollutant with the highest detection rate in aquatic environment, on PA and PLA MPs was used to evaluate the adsorption capacity of MPs and the aging characteristics of MPs under UV irradiation. The main purpose of

this research were to (1) reveal the changes of physical and chemical properties and aging mechanism of PA and PLA under simulated UV irradiation; (2) compared the adsorption properties of PA and PLA MPs for Cu(II); (3) elucidated the adsorption mechanism of Cu(II) on pristine and aged MPs; (4) investigated the effects of typical factors on the adsorption behavior of aged MPs. We expect that this work will help to better explore the interaction between aged MPs and typical heavy metal pollutants in the aquatic environment, establish the relationship between the aging performance and adsorption capacity of MPs, and provide a strong basis for the joint ecological risk assessment of aged MPs and heavy metals.

Materials and methods

Materials and reagents

PA and PLA MPs with grain diameter of approximately 50–100 μm were purchased from Guangdong Zhongcheng Plasticizing Co., Ltd. To remove metal ions and organic impurities from the MPs, the purchased MPs were first soaked in ultrapure water for 36 h, then soaked in 12% hydrochloric acid for 36 h, cleaned three times each with dehydrated ethanol and ultrapure water, and finally filtered MPs; after drying in a vacuum drying oven at 50 °C for 36 h, the MPs stored in a sample bag for further testing. The Cu(II) solution required for the experiment was prepared from $CuSO_4{\cdot}5H_2O$ purchased from Shanghai Macklin Biochemical Technology Co., Ltd., with a purity of 99.99%. Sinopharm Chemical Reagents Co., Ltd. provided the NaOH and HCl. The test vessels were immersed in 10% nitric acid for over 24 h before being flushed with ultrapure water. All chemicals used in the experiment were all analytically pure, and ultrapure water was used to prepare the solution.

Preparation of aged PA and PLA

To simulate the photo-aging process of MPs in nature, MPs were placed in a quartz tube in a photochemical reactor (XPA-1, Xujiang Electromechanical Plant, China), and mercury lamp (500 w, spectral range: 200–450 nm) was used for aging experiments. The total irradiation time of the aging process in the experiment is 240 h. For ensuring the uniformity of irradiation, MPs samples were mixed by vibration every 12 h. After aging, MPs were washed with ultrapure water and dried at 50 °C. Finally, aged PA and aged PLA were obtained, and the materials were sealed and stored for later use.

Characterization of MPs

The SSA and pore size of the MPs were determined using an automatic specific surface and porosity analyzer(BET; Micromeritics ASAP 2460, USA). A high-resolution scanning electron microscopy (SEM, ZEISS Gemini 300, Germany) was used to examine the morphology and microscopic structure of the MPs. Fourier transform infrared spectroscopy (FTIR Nicolet 5700, USA) was used to examine the functional group composition of the MPs. The crystallinity of the MPs was examined using X-ray diffraction (XRD, Rigaku Ultima IV, Japan). X-ray photoelectron spectroscopy (XPS, Thermo Scientific K-Alpha, USA) was used to determine and analyze the C1s and Cu2p of the MPs.

Batch adsorption experiments

Adsorption kinetics experiments

The influence of contacting time was used to evaluate the adsorption kinetic performance of virgin PA, aged PA, virgin PLA, and aged PLA for Cu(II). Exactly, 0.20 g MPS was added into a 50-mL brown glass bottle with 50 mL Cu(II) solution at 5.0 mg/L with the pH value at 5 which adjusted by 0.1 M HCL or NaOH. The same glass bottle was prepared in 9 for each MPs. Then, these bottles was settled into a constant temperature oscillator with 25 °C at 200 rpm/min. Each bottle was sampled only once. Preparation times of 0.25, 0.5, 1, 2, 4, 8, 12, 24, and 36 h were reached. About 5 mL solution was sampled from the bottle and then it was passed through a 0.22-μm needle filter. The filtrate was then obtained and the concentration of Cu(II) was determined using an atomic absorption spectrometer (AA320N, Instrument and Electronics Shanghai Associates). All experiments were conducted in triplicates.

Adsorption isotherm experiments

The adsorption isotherm experiments was initiated at the Cu(II) solution of 1, 2, 5, 10, and 20 mg/L in the pH value of 5 with the addition amount of 4 g/L. Adsorption equilibrium was reached at ambient temperature for 36 h in a thermostatic oscillator. After adsorption, the test samples were treated in the same manner as those used to determine the adsorption kinetics.

Influencing factors experiments

The solution was adjusted to pH 1, 2, 3, 4, 5, 6, and 7 using 0.1 mol/L HCl and NaOH to determine its impact on the adsorption by MPs. The effects of salinity were evaluated using NaCl solutions diluted to a series of various salinities (0.5, 1.0, 1.5, 2.0, 2.5, 3.0, and 3.5 wt.%). To investigate the

effect of MPs dosage, MPs were added at various densities (1.0, 2.0, 4.0, 6.0, and 8.0 g/L).

Adsorption model and statistical analysis

Data processing and statistical analyses, such as the t-test and Pearson correlation analysis of paired samples, were performed using SPSS 26.0. Origin software (version 22.0) was used for the drawing. Equation (1) was ascertained the amount of Cu(II) adsorbed on the MPs.

$$q_e = \frac{(C_0 - C_e)}{m} V \quad (1)$$

where C_0 (mg/L) and C_0 (mg/L) are the initial concentration of Cu (II) and adsorption equilibrium concentrations of Cu(II), respectively; m (g) is the mass of the added MPs; V (L) is the volume of the Cu(II) solution; and q_e (mg/g) is the adsorption capacity of Cu(II) at equilibrium.

To investigate the adsorption behavior of MPs on Cu(II), pseudo-first-order, pseudo-second-order, and intra-particle diffusion models were used to fit the kinetic data (Betianu et al. 2020; Zhang et al. 2023). The fitting equations were (2), (3), and (4).

$$q_t = q_e(1 - e^{-K_1 t}) \quad (2)$$

$$q_t = \frac{q_e^2 k_2 t}{1 + q_e k_2 t} \quad (3)$$

$$q_t = k_p t^{0.5} + C \quad (4)$$

where q_e (mg/g) is the equilibrium adsorption capacity; q_t (mg/g) is the adsorption capacity at a certain time; k_1 (h^{-1}) is the rate constant of the Lagrange pseudo-first-order adsorption reaction; k_2 ($g/(mg \bullet h)$) is the Lagrange pseudo-second-order adsorption reaction rate constant; k_p ($mg/(g \bullet h^{0.5})$) is the intra-particle diffusion rate constant; and C is a constant associated with the boundary layer's thickness.

Linear, Freundlich, and Langmuir isotherm models were used to fit the isotherm data on adsorption (Sackey et al. 2021; Zhao et al. 2013), and the expressions are shown in Eqs. (5), (6), and (7), respectively.

$$q_e = q_m \frac{K_L C_e}{1 + K_L C_e} \quad (5)$$

$$q_e = K_F C_e^{1/n} \quad (6)$$

$$q_e = K_d C_e \quad (7)$$

where q_m (mg/g) is the maximum monolayer adsorption capacity of Cu(II) on the MPs calculated using the Langmuir model, K_L (L/mg) is the adsorption constant of the Langmuir model associated with the adsorption free energy, K_F (L/mg) is the adsorption constant of the Freundlich model connected to the adsorption capacity of the MPs, 1/n is the Freundlich model constant reflecting the adsorption intensity; and K_d (L/mg) is the distribution coefficient of the linear model.

Results and discussion

Characterization of MPs

Optical and SEM morphology analysis of MPs

The apparent colors of the PA and PLA MPs after aging changed significantly from white to yellow (Fig. 1a, b, c, and d), which may have been due to the oxidation of MPs during this process, resulting in the generation of chromogenic group substances (Li et al. 2023; Liu et al. 2022b). The SEM images of the MPs before and after aging are shown in Fig. 1(e–h). The surfaces of the virgin MPs were dense, smooth, and less wrinkled, whereas those of the UV-aged MPs after UV aging was rough, accompanied by cracks, pits, and other phenomena. Changes in MPs morphology after aging may be caused by UV photooxidation degradation (Bao et al. 2022; Guo et al. 2023). In addition to stacked folds and gullies, an abundance of pore structures were found on the surface of the aged PA, which may have provided points to adsorb Cu(II) (Guo et al. 2023). The roughness of the aged MPs did not change significantly. However, some cracks appeared on the particle surface, which increased the SSA, thereby improving the pollutant adsorption capacity of the MPs. PA-MPs are more susceptible to UV irradiation in natural environments. UV radiation can cause the C–C main chains in a polymer to break and degrade, forming low-molecular-weight polymer fragments. In general, similar to previous studies, the morphology of MPs was dramatically altered by UV aging (Gao et al. 2021).

Pore structure analysis of MPs

Table 1 illustrates the differences in the SSA, pore volume, and pore diameter of the MPs before and after aging. After UV aging, the SSA of PA increased from 0.4482 to $0.6716 m^2/g$, and that of PLA increased from 0.2789 to $0.3357 m^2/g$. Compared to virgin MPs, the SSA of aged PA and PLA increased by 49.84% and 20.36%, respectively. These results show that UV irradiation leads to cracks and pits on on the surfaces of the PA and PLA MPs, which decreased the particle size and increased the SSA, which is consistent with the results of the SEM analysis. Furthermore, in comparison with virgin MPs, the pore volume and diameter increased significantly after aging. The increase in

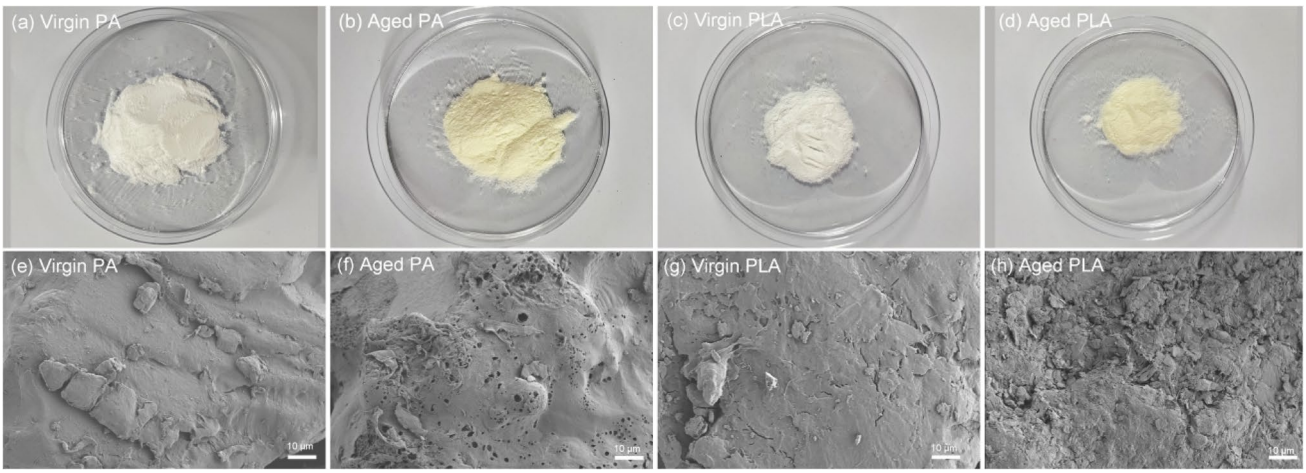

Fig. 1 Optical and SEM images of virgin and aged MPs: **a, e** virgin PA, **b, f** aged PA, **c, g** virgin PLA, and **d, h** aged PLA

Table 1 Pore structure parameters of MPs

Samples	Structure	SSA(m^2/g)	V_p(cm^3/g)	d_p(nm)
Virgin PA	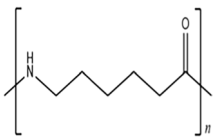	0.4482	0.000965	5.5359
Aged PA		0.6716	0.001169	6.3410
Virgin PLA	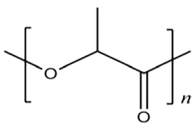	0.2789	0.000468	5.4013
Aged PLA		0.3357	0.000629	5.9536

pore volume indicates that the structure of the aged MPs was more developed and could provide more internal adsorption sites, which is consistent with previous research related to UV aging (Fan et al. 2021a). The above results show that under the action of photooxidation, the SSA of MPs increases, and the pore diameter becomes larger, which was more beneficial for the ions of heavy metals on the surface of MPs, leading to adsorption (Wang et al. 2022a).

FTIR analysis of MPs

Figure 2(a) shows the FTIR spectra of the PA MPs before and after aging. The characteristic peak at 3301 cm^{-1} corresponds to the stretching vibration of N–H on the amide group, the characteristic peak at 2935 cm^{-1} corresponds to the stretching vibration of-CH_2, the characteristic peak at 1640 cm^{-1} corresponds to the stretching vibration of C = O in the amide group, and the characteristic peak at 1541 cm^{-1} is caused by the coupling of the C-N stretching vibration and N–H bending vibration in the amide group. These are the characteristic bands of PA (Du et al. 2022; Liu et al. 2023). At these characteristic peaks, the position of the aged PA absorption peak did not change significantly, but the intensity of the absorption peak at 1640 cm^{-1} was significantly enhanced, indicating that the UV aging promoted an increase in oxygen-containing functional groups on the surface of the PA MPs. Figure 2(b) shows the FTIR spectra of

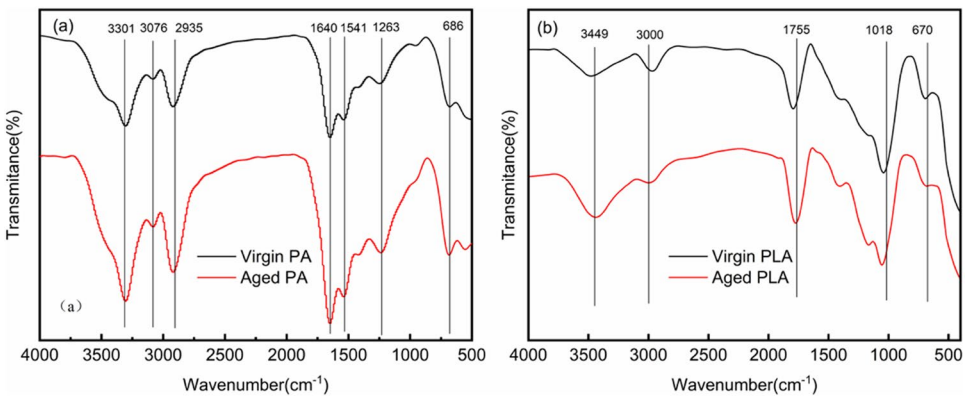

Fig. 2 FTIR spectra of virgin and aged MPs: **a** PA MPs, and **b** PLA MPs

PLA MPs before and after aging. Spectral analysis showed that the characteristic peak at 3449 cm^{-1} was the stretching vibration of O–H, the characteristic peak at 3000 cm^{-1} was the stretching vibration of-CH_2, and the characteristic peak at 1755 cm^{-1} was attributed to the stretching vibration of C = O (Fan et al. 2023; Liang et al. 2023). In comparison, the intensities of the two absorption peaks of the aged PLA at 3449 cm^{-1} and 1755 cm^{-1} were significantly enhanced, indicating that PLA underwent an oxidation reaction under UV irradiation and produced more oxygen-containing functional groups. In addition, the decreased strength of the aged PLA at 3000 cm^{-1} indicates the dissociation of C-H bonds and the formation of free radicals after aging. Studies have shown that an increase in the oxygen-containing functional groups enhances the affinity of MPs for pollutants (Li et al. 2022a), thereby promoting the adsorption of pollutants.

XRD analysis of MPs

The XRD patterns of the PA and PLA MPs before and after aging are shown in Fig. 3(a) and (b), respectively. The PA MPs exhibited sharp diffraction peaks at 20.4° and 24.2°, indicating that the ordered crystal regions of the PA MPs were regularly arranged. The position of the characteristic diffraction peak of PA MPs did not change after aging; however, the intensity of the diffraction peak decreased (Li et al. 2024, 2022a). The crystallinity analysis results showed that the crystallinity of PA MPs decreased from 69.47% to 61.02% after aging. The characteristic diffraction peak of the PLA MPs was located at 17.3°, which indicated that the crystal structure of the PLA was more orderly. After UV aging, the crystallinity of PLA MPs decreased from 77.39% to 26.25%. The decrease in crystallinity may be due to the fact that the oxidation of UV produces more oxygen-containing groups, so that some ordered structures in the polymer chains of MPs crystals are destroyed by UV light during aging, and some molecular chains undergo oxidative damage (Velzeboer et al. 2014).

Adsorption kinetics

The Cu(II) adsorption kinetics fitting curves before and after MP aging are shown in Fig. 4. The adsorption of Cu(II) on PA and PLA showed a similar trend, that is, rapid adsorption within the initial time of 1–4 h, after which the adsorption slowly reached equilibrium. As MPs have many adsorption sites, the adsorption process proceeds rapidly in the first stage. Subsequently, the MPs' surface adsorption sites were progressively filled, the adsorption rate slows down (Leng et al. 2023), and the adsorption reaches equilibrium at 36 h. The order of equilibrium adsorbability for the MPs was aged PA > aged PLA > virgin PA > virgin PLA.

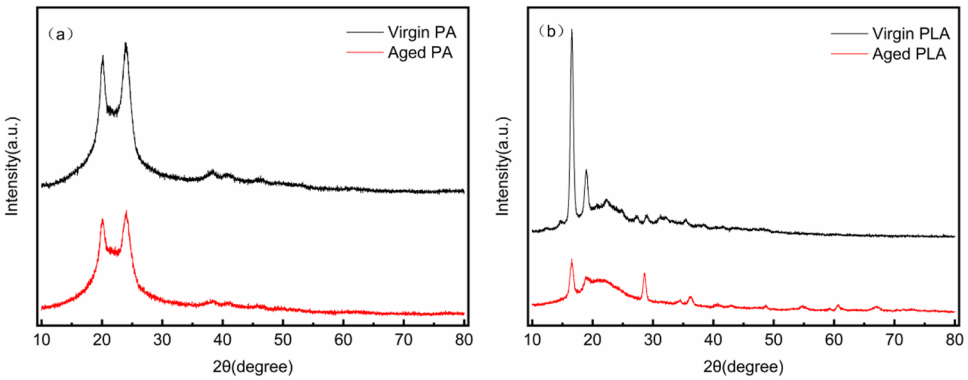

Fig. 3 XRD patterns of virgin and aged MPs: **a** PA MPs, and **b** PLA MPs

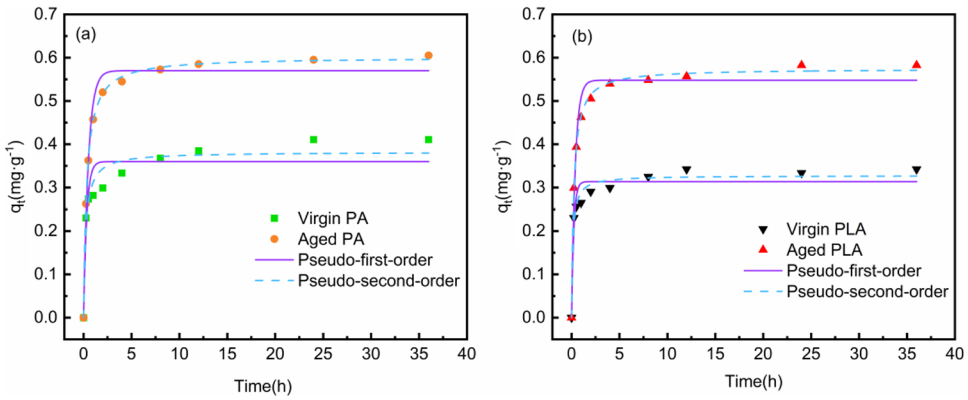

Fig. 4 The adsorption kinetics of virgin and aged MPs: **a** PA MPs, and **b** PLA MPs

Pseudo-first- and -second-order models were used to fit the kinetic data. Table 2 lists the corresponding parameters for the fitting. The findings showed that the adsorption processes of by PA and PLA were more consistent with the pseudo-second-order model, with correlation coefficients greater than 0.950. Cu(II) is mostly chemically adsorbed onto MPs by methods such as surface adsorption and external liquid film diffusion (Liu et al. 2022a). Based on the fitted rate constant and equilibrium adsorption capacity data, the UV aging treatment accelerated the process by which MPs adsorbed Cu(II) and enhanced the adsorption capacity. The adsorption capacity of aged PA and PLA to Cu(II) increased to 1.59 and 1.76 times those of virgin PA and virgin PLA, respectively. Moreover, the smaller the value, the slower the adsorption rate of MPs on heavy metal ions, and the quantity of available adsorption sites determines the adsorption rate (Han et al. 2021; Wang et al. 2020), which is similar to the SEM and SSA analysis results for MPs. Aged MPs generally have a higher adsorption rate constant than virgin MPs, indicating that aging increases the adsorption rate. This indicates that the cracks and pits on the surface of MPs caused by the aging process increased their SSA, thereby increasing the number of adsorption sites on their surfaces of MPs and improving their ability to adsorb contaminants (Fu et al. 2021).

To further clarify the adsorption of Cu(II) by the MPs before and after aging, the adsorption kinetics were investigated using an intra-particle diffusion model. Table 3 and Fig. 5 present the fitting results. There are three stages of Cu(II) adsorption on both virgin and used PA and PLA (Ma et al. 2019; Sun et al. 2023). The fitting line did not cross the origin ($C \neq 0$) in the first stage, which was the rapid adsorption stage, suggesting that there are more steps to influence the adsorption process besides intra-particle diffusion. This stage was the result of the interaction between intra-particle diffusion and surface adsorption. Intra-particle diffusion was the second stage. Cu(II) gradually permeated the interior surface of the MPs from the outer liquid sheet. The gradient of the fitting line was lower than Stage I, which was mainly due to the decrease in the intra-particle diffusion rate of the MPs caused by the decrease in the Cu(II) density of the solution. The third phase is the adsorption equilibrium

Table 2 Kinetic model parameters of Cu(II) adsorption by virgin and aged PA and PLA

Samples	Pseudo-first-order model			Pseudo-second-order model		
	$k_1(h^{-1})$	$q_e(mg/g)$	R^2	$k_2\left[g/(mg \bullet h)\right]$	$q_e(mg/g)$	R^2
Virgin PA	1.968	0.360	0.884	4.642	0.382	0.958
Aged PA	3.110	0.574	0.972	11.945	0.606	0.997
Virgin PLA	3.336	0.315	0.953	7.724	0.326	0.983
Aged PLA	2.620	0.548	0.974	16.372	0.575	0.998

Table 3 Intra-particle diffusion model parameters of Cu(II) adsorption by virgin and aged MPs

Samples	Stage I			Stage II			Stage III		
	C_1	k_{p1}	R_1^2	C_2	k_{p2}	R_2^2	C_3	k_{p3}	R_3^2
Virgin PA	0.211	0.066	0.812	0.245	0.042	0.979	0.343	0.013	0.930
Aged PA	0.152	0.275	0.938	0.478	0.032	0.980	0.557	0.007	0.994
Virgin PLA	0.205	0.061	0.950	0.251	0.026	0.985	0.338	0.002	0.987
Aged PLA	0.219	0.216	0.902	0.482	0.023	0.839	0.523	0.011	0.812

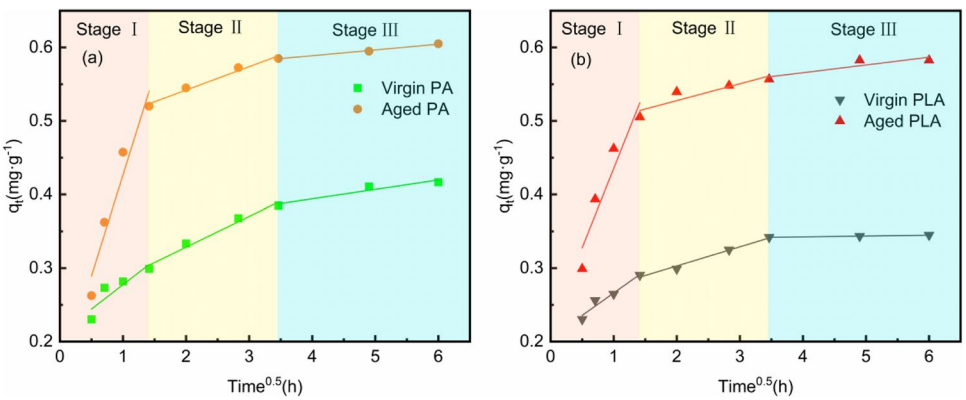

Fig. 5 Intra-particle diffusion model of Cu(II) adsorption by virgin and aged MPs: (**a**) PA MPs, and (**b**) PLA MPs

stage. The intra-particle diffusion rate continued to decline, and the residual Cu(II) density in the aquatic environment was extremely low at this point. The diffusion rate constants of the three stages of adsorption of Cu(II) by the virgin and aged PA and PLA MPs were as follows: $K_{p1} > K_{p2} > K_{p3}$, indicating that the order of the adsorption rates of the three stages was stage I > stage II > stage III. The intercept C values of the aged MPs in the three stages of adsorption were greater than those of the virgin MPs, which was mostly caused by the MPs' surfaces exhibiting more adsorption sites as they aged, increasing the mass transfer driving force of Cu(II) in MPs intra-particle diffusion (Fan et al. 2022).

Adsorption isotherms

The adsorption datum were fitted using Langmuir, Freundlich, and linear isothermal models to comprehend the adsorption properties of MPs before and after aging. The fitting results are presented in Fig. 6 and Table 4. Evidently, when the initial density of Cu(II) increased, the equilibrium adsorbability gradually increased. Comparing the three isothermal adsorption models, the R^2 values of the Langmuir and Freundlich models in the experimental analysis were higher, but the Langmuir isothermal adsorption model ($0.964 < R^2 < 0.996$) was better suited to explaining the isothermal adsorbent process of Cu(II) on PA and PLA than the Freundlich and Linear models. This indicated that the adsorption occurred on superficies of the MPs. The adsorption of Cu(II) by MPs before and after aging is mainly chemical, and the adsorption process is a monolayer adsorption (Loncarski et al. 2021). In contrast to virgin and aged MPs had a higher maximum adsorption capacity (q_m) for Cu(II), and the q_m value of the aged PA increased from 0.964 to 1.415 mg/g. Similarly, the q_m value of the PLA increased from 0.951 to 1.398 mg/g after aging, which is consistent with the kinetic process. This indicates that increasing the number of adsorption sites on the surface of the MPs following aging can enhance the ability of PA and PLA to adsorb Cu(II).

Furthermore, PA had a higher adsorption intensity and adsorption capacity for Cu(II) than PLA, both before and after aging. This is primarily because the two types of MPs exhibit different physical and chemical characteristics. Compared to the PLA MPs, the surfaces of the PA MPs contained more oxygen-functional groups, which could produce more hydrogen bonds with the surrounding water, thus enhancing the intensity of Cu(II) adsorption in water. Meanwhile, the SSA of the PA MPs was larger than PLA MPs, which gives the surface of PA MPs more adsorption sites, leading to an enhancement of the adsorption rate and capacity. In general, UV aging treatment has the potential to enhance the danger of MPs in aquatic environments while drastically altering their physical and chemical features.

Influencing factors

Effect of pH

The pH has a significant impact on the surface charge state of the MPs, the solution's concentration of heavy

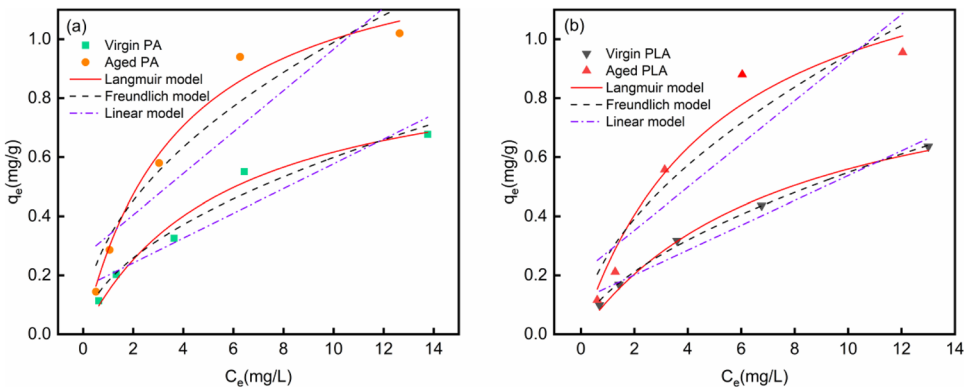

Fig. 6 The adsorption isotherm of virgin and aged MPs: **a** PA MPs, and **b** PLA MPs

Table 4 Adsorption isotherm parameters of Cu(II) adsorption by virgin and aged MPs

Samples	Langmuir model			Freundlich model			Linear model	
	$q_m(mg/g)$	$k_L(L/mg)$	R^2	n	K_F(L/mg)	R^2	$K_d(L/mg)$	R^2
Virgin PA	0.964	0.177	0.978	1.914	0.180	0.963	0.042	0.893
Aged PA	1.415	0.260	0.983	2.056	0.322	0.930	0.070	0.815
Virgin PLA	0.951	0.129	0.996	1.693	0.141	0.990	0.042	0.963
Aged PLA	1.398	0.194	0.964	1.821	0.267	0.904	0.073	0.805

metal ions, and the MPs' ability to adsorb heavy metals. The adsorption of Cu (II) by MPs in solutions with various pH values was investigated.. As shown in Fig. 7(a), the initial pH had a consistent impact on the adsorption of Cu (II) by the PA and PLA MPs, both before and after aging, which first increased and subsequently decreased as the pH value increased. At pH 5, the adsorbability achieves a maximum of 0.63 mg/g. This is because, when the pH of the solution is low, the zeta potential is positive, electrostatic repulsion is large, and the density of H^+ in the acidic environment is comparatively high. In solution, H^+ competes with Cu(II) for adsorption, and H^+ occupies the adsorption sites of the MPs, resulting in a low Cu(II) adsorption effect (Allouss et al. 2020). When the pH value exceeds 5, the increase in OH^- in the solution causes the Cu(II) to react with the OH^- in water and precipitate, which affects the adsorption of Cu(II) by MPs. In addition, compared with virgin MPs, Cu(II) has a much larger potential to bind to aged PA and PLA because aged MPs have more oxygen-functional groups and their SSA is higher.

Effects of salinity

The adsorption behavior of Cu(II) on MPs before and after aging was investigated by simulating the saline environments of rivers, estuaries, and seas using a gradient NaCl solution. According to Fig. 7(b), the adsorption capacity of Cu(II) on MPs decreased gradually when the salinity increased from 0 to 3.5%, and the effect of salinity on MPs after aging was lower than that on virgin MPs. In addition, Na^+ near the MPs may compete compete with free Cu(II) for adsorption sites on the surface of the MPs, thereby inhibiting the adsorption of Cu(II) (Wang et al. 2022b). The above discussion shows that PA and PLA MPs are more likely to enrich heavy metal pollutants in freshwater environments than in seawater.

Effect of dosage

Figure 7(c) illustrates how the MPs dosage affected Cu(II) adsorption. both before and after aging. The adsorption capacity of the MPs at equilibrium steadily decreased as the MP dosage increased from 1 to 8 g/L. Virgin PA's adsorption capacity descended from 0.68 to 0.23 mg/g, and that of virgin PLA decreased from 0.62 to 0.22 mg/g. This is because, when the original concentration and volume of the adsorbate were constant, as the dosage of the adsorbent increased, less Cu(II) was absorbed per unit mass of the adsorbent. However, Cu(II) adsorption by the MPs increased rapidly as the dosage increased. The adsorption percentages of virgin PA and PLA increased from 13.55% to 37.41% and 12.31% to 35.01%, respectively. This is mainly because, as the dosage of MPs enhanced, the adsorption sites increased, which was helpful for the adsorption of Cu(II). The adsorption capacity of MPs on Cu(II) tended to be steady at dosages greater than 4 g/L, and the adsorption rate increased slowly. This may be mainly due to the formation of large particle clusters due to the interaction between MP particles, hindering the normal diffusion of Cu(II) to the MPs' surfaces (He et al. 2020b). This causes the adsorbent particles in the solution to be overcrowded, resulting in the overlapping of adsorption binding sites and the unsaturated utilization of active binding sites during the adsorbent process (Chaturvedi et al. 2020), causing the adsorption capacity of the unit to gradually decline. In addition, the aged MPs had a larger Cu(II) adsorption capacity and adsorption rate than the virgin MPs, which is consistent with the findings of other studies.

Mechanism analysis

Physical electrostatic adsorption is a common adsorption behavior of MPs. Based on the above studies, it can be seen that the aged MPs are rougher and have a larger specific surface area than virgin MPs. These provide more adsorption sites for Cu(II) attachment to the MPs surface, which

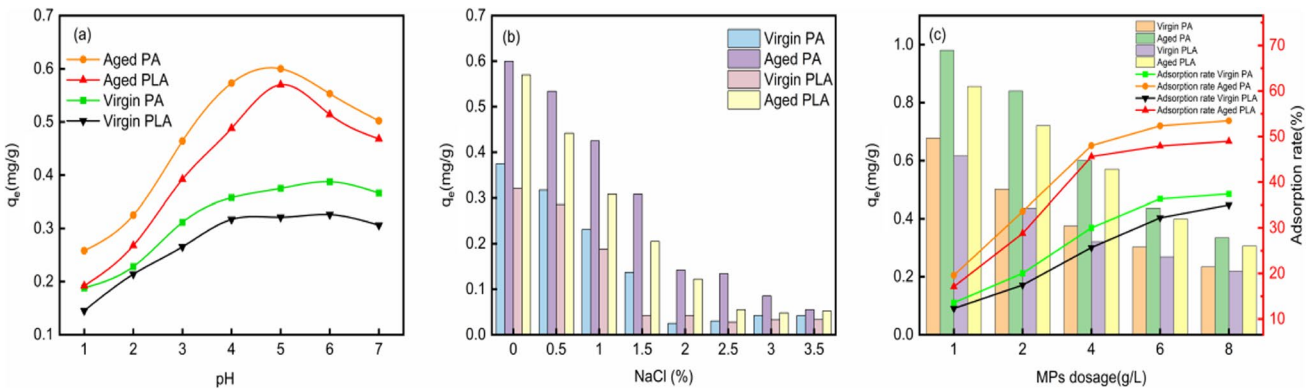

Fig. 7 Influencing factors of Cu(II) adsorption by virgin and aged MPs: **a** pH, **b** salinity, and **c** MPs dosage

is beneficial for the adsorption behavior of Cu(II) on MPs surface (Ammala et al. 2011). UV aging promotes MPs formation physical adsorption of Cu (II).

In addition, XPS spectra were used to further analyze PA and PLA before and after aging and before and after adsorption (Fig. 8a and c). It was found that the peak area of the oxygen-containing groups increased after the aging of PA and PLA, while the peak intensity corresponding to C–C decreased. The proportion of C1s peak area corresponding to C–O–C in aged PA increased from 15.82% to 19.26%, the proportion of O-C = O increased from 11.38% to 12.95%, and the proportion of C–C decreased from 72.80% to 67.79%. Similarly, the proportion of C1s peak area corresponding to C–O–C in aged PLA increased from 17.05% % to 25.39%, the proportion of O-C = O increased from 15.13% to 22.92%, and the proportion of C–C decreased from 67.80% to 51.69%. It has been proven the surface C–C of MPs is broken by UV irradiation photooxidation, and the broken unsaturated bond forms more O-C = O with O (Lang et al. 2020; Li et al. 2022b; Mao et al. 2020), which is consistent with the previous FTIR analysis results.

The XPS spectrum of Cu is shown in Fig. 8(b and d). After Cu(II) adsorption, new Cu 2p3 / 2 and Cu 2p1 / 2 peaks and satellite peaks appeared on the aged PA and PLA (Huang et al. 2017, 2024). In the Cu2p fine spectrum of aged PA after adsorption, Cu 2p1 / 2 at 954.88 eV, Cu 2p3 / 2 at 934.38 eV and a Cu satellite at 942.38 eV in aged PA. In the Cu2p fine spectrum of aged PLA after adsorption, Cu 2p1 / 2 at 952.77 eV, Cu 2p3 / 2 at 933.26 eV and a Cu satellite at 944.29 eV in aged PLA. No Cu 2p peaks were observed on the surface of the MPs prior to the adsorption of Cu(II). This result verified the chemical adsorption of Cu(II) by PA and PLA MPs. Cu(II) complexed with the functional groups of MPs and adsorbed on the surface of MPs in the form of Cu–O (Romero et al. 2015; Su et al. 2022). After adsorption, the proportion of oxygen-containing groups C–O–C and O-C = O in aged PA and PLA decreased, which once again indicated that these oxygen-containing groups were

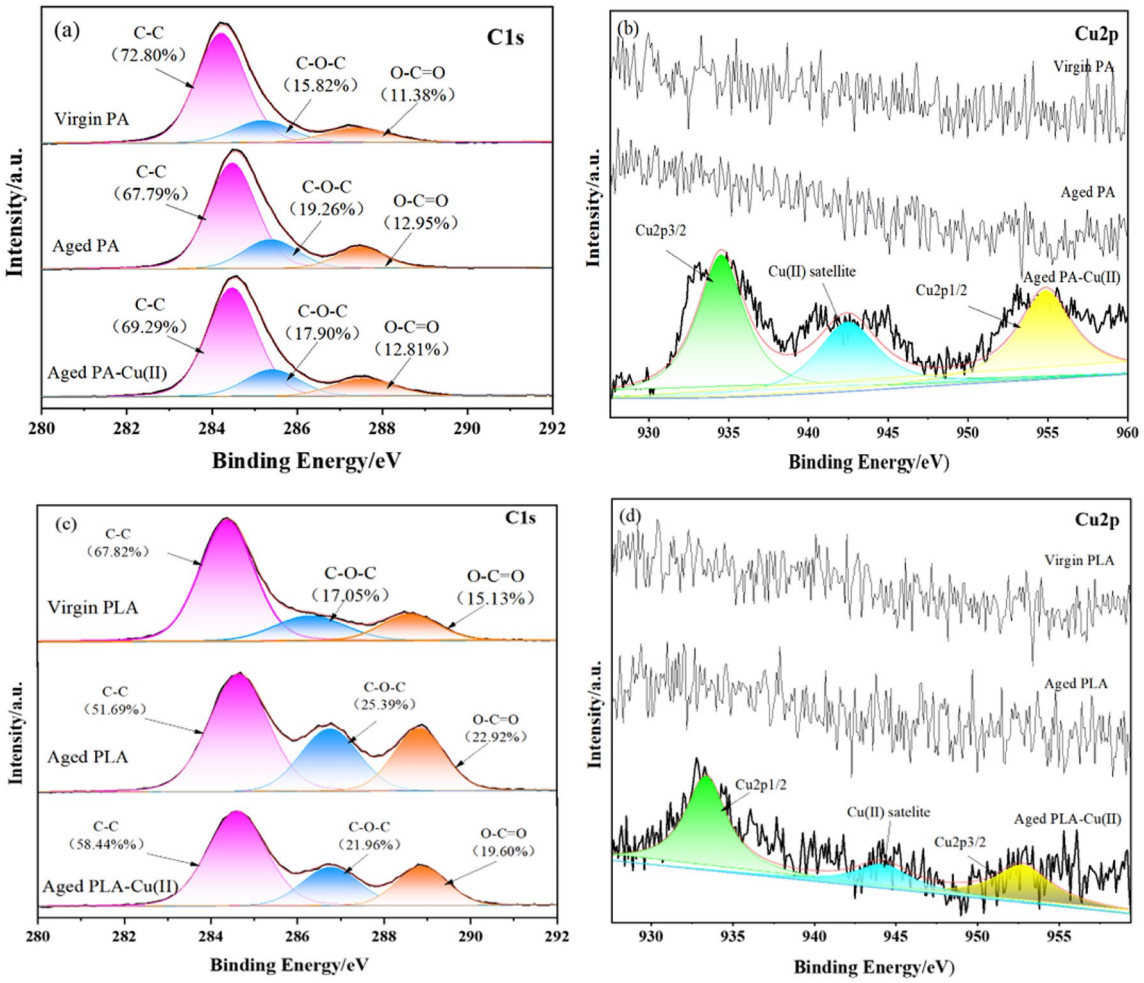

Fig. 8 XPS spectra of the PA and PLA MPs before and after adsorption of Cu(II). **a** High resolution C1s spectra of the PA; **b** Cu 2p spectra of the PA; **c** High resolution C1s spectra of the PLA; **d** Cu 2p spectra of the PLA

involved in the adsorption process of Cu(II). The reason may be that the oxygen-containing groups react with Cu(II) to form metal oxides (Arp et al. 2021; Zhou et al. 2019).

Conclusions

In this study, we investigated the adsorption behavior of two common MPs (PA and PLA) on Cu (II) before and after aging simulated by UV irradiation. The main conclusions are as follows:

(1) The UV aging process significantly changed the physical and chemical properties of PA and PLA MPs. After aging, the surface of MPs became rough, SSA increased, more oxygen-containing functional groups were produced, and the crystallinity decreased.
(2) After aging, the number of surface adsorption sites increased, thereby enhancing the adsorption capacity of MPs for Cu(II). The adsorption capacity of two kinds of virgin and aged MPs was aged PA > aged PLA > virgin PA > virgin PLA. Both the pseudo-second-order kinetic and the Langmuir models fit the experimental data well.
(3) The effects of pH and salinity on the adsorption of Cu(II) by the MPs were significant. The adsorption capacity was the highest at pH 5, and the adsorption capacity of MPs for Cu(II) decreased with increasing of salinity. The MP dosage of MPs has negativly correlated with the equilibrium adsorption capacity of Cu(II).
(4) The adsorption mechanism of Cu(II) onto MPs involves electrostatic attraction, complexation of oxygen-containing functional groups with Cu(II), and monolayer chemical adsorption.

The results of this study revealed that the aged MPs can be used as carriers, which have strong enrichment ability for heavy metal pollutants such as Cu(II), affect their migration and transformation pathways, and increase biological toxicity and ecological risks. This is of great significance for exploring the adsorption mechanism of aged MPs on heavy metals or other pollutants.

Acknowledgements The authors would like to thank all the reviewers who participated in the review and also thank to editage Editor (https://www.editage.com/) for its linguistic assistance during the preparation of this manuscript.

Author contributions Chun Hu: conceptualization, investigation, data curation, writing-original draft, writing-review and editing, project administration, and funding acquisition; Yaodong Xiao: investigation, data curation, formal analysis, and writing-original draft; Qingrong Jiang: investigation, and data curation; Mengyao Wang: investigation, and writing-review and editing; Tingdan Xue: investigation and conceptualization.

Funding This study was supported by National Natural Science Foundation of China (31270215) and Research Project of Hubei Provincial Department of Education (15Q119, and Q20131708).

Data availability Not applicable.

Declarations

Ethics approval and consent to participate Not applicable.

Consent for publication Not applicable.

Competing interests The authors have no relevant financial or non-financial interests to disclose.

References

Ahechti M, Benomar M, El Alami M, Mendiguchía C (2022) Metal adsorption by microplastics in aquatic environments under controlled conditions: exposure time, pH and salinity. Int J Environ Anal Chem 102:1118–1125. https://doi.org/10.1080/03067319.2020.1733546

Alimi OS, Budarz JF, Hernandez LM, Tufenkji N (2018) Microplastics and Nanoplastics in Aquatic Environments: Aggregation, Deposition, and Enhanced Contaminant Transport. Environ Sci Technol 52:1704–1724. https://doi.org/10.1021/acs.est.7b05559

Allouss D, Essamlali Y, Chakir A, Khadhar S, Zahouily M (2020) Effective removal of Cu(II) from aqueous solution over graphene oxide encapsulated carboxymethylcellulose-alginate hydrogel microspheres: towards real wastewater treatment plants. Environ Sci Pollut Res 27:7476–7492. https://doi.org/10.1007/s11356-019-06950-w

Ammala A, Bateman S, Dean K, Petinakis E, Sangwan P, Wong S, Yuan Q, Yu L, Patrick C, Leong KH (2011) An overview of degradable and biodegradable polyolefins. Prog Polym Sci 36:1015–1049. https://doi.org/10.1016/j.progpolymsci.2010.12.002

Arp HPH, Kühnel D, Rummel C, MacLeod M, Potthoff A, Reichelt S, Rojo-Nieto E, Schmitt-Jansen M, Sonnenberg J, Toorman E, Jahnke A (2021) Weathering Plastics as a Planetary Boundary Threat: Exposure, Fate, and Hazards. Environ Sci Technol 55:7246–7255. https://doi.org/10.1021/acs.est.1c01512

Bao RQ, Fu DD, Fan ZQ, Peng XZ, Peng LC (2022) Aging of microplastics and their role as vector for copper in aqueous solution. Gondwana Res 108:81–90. https://doi.org/10.1016/j.gr.2021.12.002

Bergmann M, Mützel S, Primpke S, Tekman MB, Trachsel J, Gerdts G (2019) White and wonderful? Microplastics prevail in snow from the Alps to the Arctic. Sci Adv 5:10. https://doi.org/10.1126/sciadv.aax1157

Betianu CS, Cozma P, Rosca M, Ungureanu EDC, Mamaliga I, Gavrilescu M (2020) Sorption of Organic Pollutants onto Soils: Surface Diffusion Mechanism of Congo Red Azo Dye. Processes 8:19. https://doi.org/10.3390/pr8121639

Brennecke D, Duarte B, Paiva F, Caçador I, Canning-Clode J (2016) Microplastics as vector for heavy metal contamination from the marine environment. Estuar Coast Shelf Sci 178:189–195. https://doi.org/10.1016/j.ecss.2015.12.003

Carbery M, O'Connor W, Thavamani P (2018) Trophic transfer of microplastics and mixed contaminants in the marine food web

and implications for human health. Environ Int 115:400–409. https://doi.org/10.1016/j.envint.2018.03.007
Chaturvedi G, Kaur A, Umar A, Khan MA, Algarni H, Kansal SK (2020) Removal of fluoroquinolone drug, levofloxacin, from aqueous phase over iron based MOFs, MIL-100(Fe). J Solid State Chem 281:10. https://doi.org/10.1016/j.jssc.2019.121029
Chen LY, Liu WX, Yang T, Nowack B (2023) Probabilistic material flow analysis of eight commodity plastics in China: Comparison between 2017 and 2020. Resour Conserv Recycl 191:14. https://doi.org/10.1016/j.resconrec.2023.106880
Cherono F, Mburu N, Kakoi B (2021) Adsorption of lead, copper and zinc in a multi-metal aqueous solution by waste rubber tires for the design of single batch adsorber. Heliyon 7:12. https://doi.org/10.1016/j.heliyon.2021.e08254
Cole M, Lindeque P, Halsband C, Galloway TS (2011) Microplastics as contaminants in the marine environment: A review. Mar Pollut Bull 62:2588–2597. https://doi.org/10.1016/j.marpolbul.2011.09.025
Crespo M, Gómez-del Río T, Rodríguez J (2019) Failure of polyamide 12 notched samples manufactured by selective laser sintering. J Strain Anal Eng Des 54:192–198. https://doi.org/10.1177/0309324719847817
De Gisi S, Gadaleta G, Gorrasi G, La Mantia FP, Notarnicola M, Sorrentino A (2022) The role of (bio)degradability on the management of petrochemical and bio-based plastic waste. J Environ Manage 310:16. https://doi.org/10.1016/j.jenvman.2022.114769
Ding JF, Ju P, Ran Q, Li JX, Jiang FH, Cao W, Zhang J, Sun CJ (2023) Elder fish means more microplastics? Alaska pollock microplastic story in the Bering Sea. Sci Adv 9:10. https://doi.org/10.1126/sciadv.adf5897
Dong JW, Xia XH, Liu ZX, Zhang XT, Chen QW (2019) Variations in concentrations and bioavailability of heavy metals in rivers during sediment suspension-deposition event induced by dams: insights from sediment regulation of the Xiaolangdi Reservoir in the Yellow River. J Soils Sediments 19:403–414. https://doi.org/10.1007/s11368-018-2016-1
Du S, Wei YH, Ahmed S, Zhou FY, Tan YH, Li Y, Wang M, Chen XX, Zhou WT (2022) Enhanced thermal stability and UV resistance of polyamide 6 filament fabric *via in-situ* grafting with methyl methacrylate. Colloid Surf A-Physicochem Eng Asp 651:9. https://doi.org/10.1016/j.colsurfa.2022.129371
Fan XL, Gan R, Liu JQ, Xie Y, Xu DZ, Xiang Y, Su JK, Teng Z, Hou J (2021a) Adsorption and desorption behaviors of antibiotics by tire wear particles and polyethylene microplastics with or without aging processes. Sci Total Environ 771:10. https://doi.org/10.1016/j.scitotenv.2021.145451
Fan XL, Zou YF, Geng N, Liu JQ, Hou J, Li DD, Yang CF, Li Y (2021b) Investigation on the adsorption and desorption behaviors of antibiotics by degradable MPs with or without UV ageing process. J Hazard Mater 401:11. https://doi.org/10.1016/j.jhazmal.2020.123363
Fan XL, Shi S, Xiang Y, Xie Y, Chen Q, Yang YY, Liu JQ, Zhang JK, Hou J (2022) Insights into the Characteristics, Adsorption, and Desorption Behaviors of Polylactic Acid Aged with or without Salinities. J Environ Eng-ASCE 148.https://doi.org/10.1061/(asce)ee.1943-7870.0002025
Fan XL, Xie Y, Qian SW, Xiang Y, Chen Q, Yang YY, Liu JQ, Zhang JK, Hou J (2023) Insights into the characteristics, adsorption and desorption behaviors of microplastics aged with or without fulvic acid. Environ Sci Pollut Res 30:10484–10494. https://doi.org/10.1007/s11356-022-22897-x
Fiore M, Garofalo SF, Migliavacca A, Mansutti A, Fino D, Tommasi T (2022) Tackling Marine Microplastics Pollution: an Overview of Existing Solutions. Water Air Soil Pollut 233:21. https://doi.org/10.1007/s11270-022-05715-5
Foshtomi MY, Oryan S, Taheri M, Bastami KD, Zahed MA (2019) Composition and abundance of microplastics in surface sediments and their interaction with sedimentary heavy metals, PAHs and TPH (total petroleum hydrocarbons). Mar Pollut Bull 149:7. https://doi.org/10.1016/j.marpolbul.2019.110655
Fu QM, Tan XF, Ye SJ, Ma LL, Gu YL, Zhang P, Chen Q, Yang YY, Tang YQ (2021) Mechanism analysis of heavy metal lead captured by natural-aged microplastics. Chemosphere 270:9. https://doi.org/10.1016/j.chemosphere.2020.128624
Gao L, Fu DD, Zhao JJ, Wu WS, Wang ZZ, Su YY, Peng LC (2021) Microplastics aged in various environmental media exhibited strong sorption to heavy metals in seawater. Mar Pollut Bull 169:11. https://doi.org/10.1016/j.marpolbul.2021.112480
Geng Y, He H, Liu H, Jing HS (2020) Preparation of polycarbonate/poly(lactic acid) with improved printability and processability for fused deposition modeling. Polym Adv Technol 31:2848–2862. https://doi.org/10.1002/pat.5013
Guo CX, Wang LL, Lang DN, Qian QQ, Wang W, Wu RL, Wang JD (2023) UV and chemical aging alter the adsorption behavior of microplastics for tetracycline. Environ Pollut 318:10. https://doi.org/10.1016/j.envpol.2022.120859
Guo X, Wang JL (2019) The chemical behaviors of microplastics in marine environment: A review. Mar Pollut Bull 142:1–14. https://doi.org/10.1016/j.marpolbul.2019.03.019
Han XX, Wang SY, Yu X, Vogt RD, Feng JF, Zhai LF, Ma WQ, Zhu L, Lu XQ (2021) Kinetics and Size Effects on Adsorption of Cu(II), Cr(III), and Pb(II) Onto Polyethylene, Polypropylene, and Polyethylene Terephthalate Microplastic Particles. Front Mar Sci 8:6. https://doi.org/10.3389/fmars.2021.785146
He WT, Yu QD, Wang N, Ouyang XK (2020a) Efficient adsorption of Cu(II) from aqueous solutions by acid-resistant and recyclable ethylenediamine tetraacetic acid-grafted polyvinyl alcohol/chitosan beads. J Mol Liq 316:10. https://doi.org/10.1016/j.molliq.2020.113856
He XP, Yao B, Xia Y, Huang H, Gan YP, Zhang WK (2020b) Coal fly ash derived zeolite for highly efficient removal of Ni^{2+} in waste water. Powder Technol 367:40–46. https://doi.org/10.1016/j.powtec.2019.11.037
Hu MF, Hou N, Li YF, Liu YM, Zhang H, Zeng DQ, Tan HH (2021) The effect of microplastics on behaviors of chiral imidazolinone herbicides in the aquatic environment: Residue, degradation and distribution. J Hazard Mater 418:12. https://doi.org/10.1016/j.jhazmat.2021.126176
Huang BY, Liu YG, Li B, Liu SB, Zeng GM, Zeng ZW, Wang XH, Ning QM, Zheng BH, Yang CP (2017) Effect of Cu(II) ions on the enhancement of tetracycline adsorption by Fe_3O_4@SiO_2-Chitosan/graphene oxide nanocomposite. Carbohydr Polym 157:576–585. https://doi.org/10.1016/j.carbpol.2016.10.025
Huang W, Zhang J, Zhang Z, Gao H, Xu W, Xia X (2024) Insights into adsorption behavior and mechanism of Cu(II) onto biodegradable and conventional microplastics: Effect of aging process and environmental factors. Environ Pollut 342:123061. https://doi.org/10.1016/j.envpol.2023.123061
Jang M, Shim WJ, Cho Y, Han GM, Song YK, Hong SH (2020) A close relationship between microplastic contamination and coastal area use pattern. Water Res 171:10. https://doi.org/10.1016/j.watres.2019.115400
Kalcíková G, Skalar T, Marolt G, Kokalj AJ (2020) An environmental concentration of aged microplastics with adsorbed silver significantly affects aquatic organisms. Water Res 175:9. https://doi.org/10.1016/j.watres.2020.115644
Kataoka T, Nihei Y, Kudou K, Hinata H (2019) Assessment of the sources and inflow processes of microplastics in the river environments of Japan. Environ Pollut 244:958–965. https://doi.org/10.1016/j.envpol.2018.10.111

Khalid N, Aqeel M, Noman A, Khan SM, Akhter N (2021) Interactions and effects of microplastics with heavy metals in aquatic and terrestrial environments. Environ Pollut 290:13. https://doi.org/10.1016/j.envpol.2021.118104

Lang MF, Yu XQ, Liu JH, Xia TJ, Wang TC, Jia HZ, Guo XT (2020) Fenton aging signi ficantly affects the heavy metal adsorption capacity of polystyrene microplastics. Sci Total Environ 722:9. https://doi.org/10.1016/j.scitotenv.2020.137762

Leng YF, Wang W, Cai HP, Chang FY, Xiong W, Wang J (2023) Sorption kinetics, isotherms and molecular dynamics simulation of 17β-estradiol onto microplastics. Sci Total Environ 858:8. https://doi.org/10.1016/j.scitotenv.2022.159803

Li CR, Busquets R, Campos LC (2020) Assessment of microplastics in freshwater systems: A review. Sci Total Environ 707:12. https://doi.org/10.1016/j.scitotenv.2019.135578

Li J, Yu SG, Cui M (2023) Aged polyamide microplastics enhance the adsorption of trimethoprim in soil environments. Environ Monit Assess 195:13. https://doi.org/10.1007/s10661-023-11350-2

Li JY, Liu HH, Chen JP (2018) Microplastics in freshwater systems: A review on occurrence, environmental effects, and methods for microplastics detection. Water Res 137:362–374. https://doi.org/10.1016/j.watres.2017.12.056

Li L, Xue B, Lin H, Lan W, Wang X, Wei J, Li M, Li M, Duan Y, Lv J, Chen Z (2024) The adsorption and release mechanism of different aged microplastics toward Hg(II) via batch experiment and the deep learning method. Chemosphere 350:141067. https://doi.org/10.1016/j.chemosphere.2023.141067

Li SS, Ma RX, Zhu XH, Liu C, Li LZ, Yu ZL, Chen XC, Li ZR, Yang Y (2021) Sorption of tetrabromobisphenol A onto microplastics: Behavior, mechanisms, and the effects of sorbent and environmental factors. Ecotox Environ Safe 210:7. https://doi.org/10.1016/j.ecoenv.2020.111842

Li YC, Wang JZ, Xue BQ, Wang SH, Qi P, Sun J, Li HF, Gu XY, Zhang S (2022a) Enhancing the flame retardancy and UV resistance of polyamide 6 by introducing ternary supramolecular aggregates. Chemosphere 287:10. https://doi.org/10.1016/j.chemosphere.2021.132100

Li YH, Zhang Y, Su F, Wang YY, Peng LL, Liu DZ (2022b) Adsorption behaviour of microplastics on the heavy metal Cr(VI) before and after ageing. Chemosphere 302:9. https://doi.org/10.1016/j.chemosphere.2022.134865

Liang JN, Wu JH, Zeng Z, Li MZ, Liu WZ, Zhang TP (2023) Behavior and mechanisms of ciprofloxacin adsorption on aged polylactic acid and polyethlene microplastics. Environ Sci Pollut Res 30:62938–62950. https://doi.org/10.1007/s11356-023-26390-x

Lionetto F, Corcione CE, Messa F, Perrone S, Salomone A, Maffezzoli A (2023) The Sorption of Amoxicillin on Engineered Polyethylene Terephthalate Microplastics. J Polym Environ 31:1383–1397. https://doi.org/10.1007/s10924-022-02690-0

Liu H, Zhang X, Ji B, Qiang ZM, Karanfil T, Liu C (2023) UV aging of microplastic polymers promotes their chemical transformation and byproduct formation upon chlorination. Sci Total Environ 858:10. https://doi.org/10.1016/j.scitotenv.2022.159842

Liu P, Qian L, Wang HY, Zhan X, Lu K, Gu C, Gao SX (2019) New Insights into the Aging Behavior of Microplastics Accelerated by Advanced Oxidation Processes. Environ Sci Technol 53:3579–3588. https://doi.org/10.1021/acs.est.9b00493

Liu P, Lu K, Li JL, Wu XW, Qian L, Wang MJ, Gao SX (2020) Effect of aging on adsorption behavior of polystyrene microplastics for pharmaceuticals: Adsorption mechanism and role of aging intermediates. J Hazard Mater 384:9. https://doi.org/10.1016/j.jhazmat.2019.121193

Liu X, Zhou DD, Chen M, Cao YW, Zhuang LY, Lu ZH, Yang ZH (2022a) Adsorption behavior of azole fungicides on polystyrene and polyethylene microplastics. Chemosphere 308:9. https://doi.org/10.1016/j.chemosphere.2022.136280

Liu XW, Zheng MG, Wang L, Ke RH, Lou YH, Zhang XJ, Dong XF, Zhang Y (2018) Sorption behaviors of tris-(2,3-dibromopropyl) isocyanurate and hexabromocyclododecanes on polypropylene microplastics. Mar Pollut Bull 135:581–586. https://doi.org/10.1016/j.marpolbul.2018.07.061

Liu YX, Zhang J, Cao WG, Hu Y, Shen WB (2022b) The influence of Pb(II) adsorption on (Non) biodegradable microplastics by UV/O_3 oxidation treatment. J Environ Chem Eng 10:11. https://doi.org/10.1016/j.jece.2022.108615

Loncarski M, Gvoic V, Prica M, Cveticanin L, Agbaba J, Tubic A (2021) Sorption behavior of polycyclic aromatic hydrocarbons on biodegradable polylactic acid and various nondegradable microplastics: Model fitting and mechanism analysis. Sci Total Environ 785:13. https://doi.org/10.1016/j.scitotenv.2021.147289

Luo HW, Liu CY, He DQ, Xu J, Sun JQ, Li J, Pan XL (2022) Environmental behaviors of microplastics in aquatic systems: A systematic review on degradation, adsorption, toxicity and biofilm under aging conditions. J Hazard Mater 423:16. https://doi.org/10.1016/j.jhazmat.2021.126915

Luo HW, Tu CL, He DQ, Zhang AP, Sun JQ, Li J, Xu J, Pan XL (2023) Interactions between microplastics and contaminants: A review focusing on the effect of aging process. Sci Total Environ 899:14. https://doi.org/10.1016/j.scitotenv.2023.165615

Lv MJ, Jiang B, Xing Y, Ya HB, Zhang T, Wang X (2022) Recent advances in the breakdown of microplastics: strategies and future prospectives. Environ Sci Pollut Res 29:65887–65903. https://doi.org/10.1007/s11356-022-22004-0

Ma J, Zhao JH, Zhu ZL, Li LQ, Yu F (2019) Effect of microplastic size on the adsorption behavior and mechanism of triclosan on polyvinyl chloride. Environ Pollut 254:10. https://doi.org/10.1016/j.envpol.2019.113104

Mao RF, Lang MF, Yu XQ, Wu RR, Yang XM, Guo XT (2020) Aging mechanism of microplastics with UV irradiation and its effects on the adsorption of heavy metals. J Hazard Mater 393:10. https://doi.org/10.1016/j.jhazmat.2020.122515

Marsic-Lucic J, Lusic J, Tutman P, Bojanic Varezic D, Siljic J, Pribudic J (2018) Levels of trace metals on microplastic particles in beach sediments of the island of Vis, Adriatic Sea. Croatia Mar Pollut Bull 137:231–236. https://doi.org/10.1016/j.marpolbul.2018.10.027

Mejías C, Martín J, Santos JL, Aparicio I, Alonso E (2023) Role of polyamide microplastics as vector of parabens in the environment: An adsorption study. Environ Technol Innov 32:13. https://doi.org/10.1016/j.eti.2023.103276

Naji A, Azadkhah S, Farahani H, Uddin S, Khan FR (2021) Microplastics in wastewater outlets of Bandar Abbas city (Iran): A potential point source of microplastics into the Persian Gulf. Chemosphere 262:8. https://doi.org/10.1016/j.chemosphere.2020.128039

Napper IE, Bakir A, Rowland SJ, Thompson RC (2015) Characterisation, quantity and sorptive properties of microplastics extracted from cosmetics. Mar Pollut Bull 99:178–185. https://doi.org/10.1016/j.marpolbul.2015.07.029

O'Connor D, Hou DY, Ok YS, Lanphear BP (2020) The effects of iniquitous lead exposure on health. Nat Sustain 3:77–79. https://doi.org/10.1038/s41893-020-0475-z

Obbard RW, Sadri S, Wong YQ, Khitun AA, Baker I, Thompson RC (2014) Global warming releases microplastic legacy frozen in Arctic Sea ice. Earth Future 2:315–320. https://doi.org/10.1002/2014ef000240

Oni BA, Ayeni AO, Agboola O, Oguntade T, Obanla O (2020) Comparing microplastics contaminants in (dry and raining) seasons for Ox-Bow Lake in Yenagoa Nigeria. Ecotox Environ Safe 198:8. https://doi.org/10.1016/j.ecoenv.2020.110656

Oni BA, Sanni SE (2022) Occurrence of Microplastics in Borehole Drinking Water and Sediments in Lagos. Nigeria Environ Toxicol Chem 41:1721–1731. https://doi.org/10.1002/etc.5350

Petersen F, Hubbart JA (2021) The occurrence and transport of microplastics: The state of the science. Sci Total Environ 758:12. https://doi.org/10.1016/j.scitotenv.2020.143936

Rahman A, Sarkar A, Yadav OP, Achari G, Slobodnik J (2021) Potential human health risks due to environmental exposure to nano-and microplastics and knowledge gaps: A scoping review. Sci Total Environ 757:13. https://doi.org/10.1016/j.scitotenv.2020.143872

Reinaldo JS, Pereira LM, Silva ES, Macedo TCP, Damasceno IZ, Ito EN (2020) Thermal, mechanical and morphological properties of multicomponent blends based on acrylic and styrenic polymers. Polym Test 82:9. https://doi.org/10.1016/j.polymertesting.2019.106265

Rochman CM, Hoh E, Hentschel BT, Kaye S (2013) Long-Term Field Measurement of Sorption of Organic Contaminants to Five Types of Plastic Pellets: Implications for Plastic Marine Debris. Environ Sci Technol 47:1646–1654. https://doi.org/10.1021/es303700s

Romero D, Chlala D, Labaki M, Royer S, Bellat JP, Bezverkhyy I, Giraudon JM, Lamonier JF (2015) Removal of Toluene over NaX Zeolite Exchanged with Cu^{2+}. Catalysts 5:1479–1497. https://doi.org/10.3390/catal5031479

Rubio L, Marcos R, Hernández A (2020) Potential adverse health effects of ingested micro- and nanoplastics on humans. Lessons learned from in vivo and in vitro mammalian models. J Toxicol Env Health-Pt b-Crit Rev. 23:51–68. https://doi.org/10.1080/10937404.2019.1700598

Sackey EA, Song YL, Yu Y, Zhuang HF (2021) Biochars derived from bamboo and rice straw for sorption of basic red dyes. PLoS ONE 16:20. https://doi.org/10.1371/journal.pone.0254637

Shen XC, Li DC, Sima XF, Cheng HY, Jiang H (2018) The effects of environmental conditions on the enrichment of antibiotics on microplastics in simulated natural water column. Environ Res 166:377–383. https://doi.org/10.1016/j.envres.2018.06.034

Sheng DR, Meng XH, Wen XH, Wu J, Yu HJ, Wu M (2022) Contamination characteristics, source identification, and source-specific health risks of heavy metal(loid)s in groundwater of an arid oasis region in Northwest China. Sci Total Environ 841:15. https://doi.org/10.1016/j.scitotenv.2022.156733

Su XY, Chen Y, Li YF, Li J, Song W, Li XG, Yan LG (2022) Enhanced adsorption of aqueous Pb(II) and Cu(II) by biochar loaded with layered double hydroxide: Crucial role of mineral precipitation. J Mol Liq 357:9. https://doi.org/10.1016/j.molliq.2022.119083

Sun C, Wei SY, Tan HY, Huang YL, Zhang YH (2022) Progress in upcycling polylactic acid waste as an alternative carbon source: A review. Chem Eng J 446:21. https://doi.org/10.1016/j.cej.2022.136881

Sun Y, Peng BY, Wang Y, Wang XJ, Xia SQ, Zhao JF (2023) Evaluating the adsorption and desorption performance of poly(butylene adipate-*co*-terephthalate) (PBAT) microplastics towards Cu(II): The roles of biofilms and biodegradation. Chem Eng J 464:13. https://doi.org/10.1016/j.cej.2023.142714

Tan DJ, Bilal GS, Komal B (2020) Impact of Carbon Emission Trading System Participation and Level of Internal Control on Quality of Carbon Emission Disclosures: Insights from Chinese State-Owned Electricity Companies. Sustainability 12:14. https://doi.org/10.3390/su12051788

Thompson RC, Olsen Y, Mitchell RP, Davis A, Rowland SJ, John AWG, McGonigle D, Russell AE (2004) Lost at sea: Where is all the plastic? Science 304:838–838. https://doi.org/10.1126/science.1094559

Torres FG, Dioses-Salinas DC, Pizarro-Ortega CI, De-la-Torre GE (2021) Sorption of chemical contaminants on degradable and non-degradable microplastics: Recent progress and research trends. Sci Total Environ 757:14. https://doi.org/10.1016/j.scitotenv.2020.143875

Upadhyay R, Singh S, Kaur G (2022) Sorption of pharmaceuticals over microplastics' surfaces: interaction mechanisms and governing factors. Environ Monit Assess 194:15. https://doi.org/10.1007/s10661-022-10475-0

Velusamy S, Roy A, Sundaram S, Mallick TK (2021) A Review on Heavy Metal Ions and Containing Dyes Removal Through Graphene Oxide-Based Adsorption Strategies for Textile Wastewater Treatment. Chem Rec 21:1570–1610. https://doi.org/10.1002/tcr.202000153

Velzeboer I, Kwadijk C, Koelmans AA (2014) Strong Sorption of PCBs to Nanoplastics, Microplastics, Carbon Nanotubes, and Fullerenes. Environ Sci Technol 48:4869–4876. https://doi.org/10.1021/es405721v

Wang CH, Zhao J, Xing BS (2021a) Environmental source, fate, and toxicity of microplastics. J Hazard Mater 407:17. https://doi.org/10.1016/j.jhazmat.2020.124357

Wang H, Qiu C, Song YL, Bian SC, Wang Q, Chen YM, Fang CR (2022a) Adsorption of tetracycline and Cd(II) on polystyrene and polyethylene terephthalate microplastics with ultraviolet and hydrogen peroxide aging treatment. Sci Total Environ 845:11. https://doi.org/10.1016/j.scitotenv.2022.157109

Wang LL, Guo CX, Qian QQ, Lang DN, Wu RL, Abliz S, Wang W, Wang JD (2023) Adsorption behavior of UV aged microplastics on the heavy metals Pb(II) and Cu(II) in aqueous solutions. Chemosphere 313:12. https://doi.org/10.1016/j.chemosphere.2022.137439

Wang QJ, Zhang Y, Wangjin XX, Wang YL, Meng GH, Chen YH (2020) The adsorption behavior of metals in aqueous solution by microplastics effected by UV radiation. J Environ Sci 87:272–280. https://doi.org/10.1016/j.jes.2019.07.006

Wang SW, Zhong S, Zheng XY, Xiao D, Zheng LL, Yang Y, Zhang HD, Ai BL, Sheng ZW (2021b) Calcite modification of agricultural waste biochar highly improves the adsorption of Cu(II) from aqueous solutions. J Environ Chem Eng 9:10. https://doi.org/10.1016/j.jece.2021.106215

Wang XX, Zhang RX, Li ZY, Yan B (2022b) Adsorption properties and influencing factors of Cu(II) on polystyrene and polyethylene terephthalate microplastics in seawater. Sci Total Environ 812:12. https://doi.org/10.1016/j.scitotenv.2021.152573

Wang ZZ, Fu DD, Gao L, Qi HY, Su YY, Peng LC (2021c) Aged microplastics decrease the bioavailability of coexisting heavy metals to microalga Chlorella vulgaris. Ecotox Environ Safe 217:9. https://doi.org/10.1016/j.ecoenv.2021.112199

Wright SL, Thompson RC, Galloway TS (2013) The physical impacts of microplastics on marine organisms: A review. Environ Pollut 178:483–492. https://doi.org/10.1016/j.envpol.2013.02.031

Wu TF, Zhu GW, Chen JH, Yang TT (2020) *In-situ* observations of internal dissolved heavy metal release in relation to sediment suspension in lake Taihu China. J Environ Sci 97:120–131. https://doi.org/10.1016/j.jes.2020.05.004

Xie FY, Yu MC, Yuan QK, Meng Y, Qie YK, Shang ZM, Luan FB, Zhang DL (2022) Spatial distribution, pollution assessment, and source identification of heavy metals in the Yellow River. J Hazard Mater 436:12. https://doi.org/10.1016/j.jhazmat.2022.129309

Yan MT, Nie HY, Xu KH, He YH, Hu YT, Huang YM, Wang J (2019) Microplastic abundance, distribution and composition in the Pearl River along Guangzhou city and Pearl River estuary, China. Chemosphere 217:879–886. https://doi.org/10.1016/j.chemosphere.2018.11.093

Zhang GY, Yang ZC, Teng Q, Han YQ, Zhang SH, Liu SY (2023) Adsorption of Pb (II) and Cu (II) by magnetic beads loaded with xanthan gum. Environ Sci Pollut Res 30:33624–33635. https://doi.org/10.1007/s11356-022-24620-2

Zhang K, Xiong X, Hu HJ, Wu CX, Bi YH, Wu YH, Zhou BS, Lam PKS, Liu JT (2017) Occurrence and Characteristics of Microplastic Pollution in Xiangxi Bay of Three Gorges Reservoir.

China Environ Sci Technol 51:3794–3801. https://doi.org/10.1021/acs.est.7b00369

Zhao JM, Ran W, Teng J, Liu YL, Liu H, Yin XN, Cao RW, Wang Q (2018) Microplastic pollution in sediments from the Bohai Sea and the Yellow Sea. China Sci Total Environ 640:637–645. https://doi.org/10.1016/j.scitotenv.2018.05.346

Zhao YX, Yang YN, Yang SJ, Wang QH, Feng CP, Zhang ZY (2013) Adsorption of high ammonium nitrogen from wastewater using a novel ceramic adsorbent and the evaluation of the ammonium-adsorbed-ceramic as fertilizer. J Colloid Interface Sci 393:264–270. https://doi.org/10.1016/j.jcis.2012.10.028

Zhou YY, He YZ, Xiang YJ, Meng SJ, Liu XC, Yu JF, Yang J, Zhang JC, Qin PF, Luo L (2019) Single and simultaneous adsorption of pefloxacin and Cu(II) ions from aqueous solutions by oxidized multiwalled carbon nanotube. Sci Total Environ 646:29–36. https://doi.org/10.1016/j.scitotenv.2018.07.267

Zhuang ST, Wang JL (2023) Interaction between antibiotics and microplastics: Recent advances and perspective. Sci Total Environ 897:17. https://doi.org/10.1016/j.scitotenv.2023.165414